Synthesis, Structure, and Magnetic Properties of a New Chloro-Bridged Dimer $[Cu_2(dpt)_2Cl_2]Cl_2$ with an Unusual Structure and Ferromagnetic Coupling

Montserrat Rodríguez and Antoni Llobet*

Departament de Química, Universitat de Girona, Campus de Montilivi 17071, Girona, Spain

Montserrat Corbella*

Departament de Química Inorgànica, Universitat de Barcelona, Martí i Franquès, 1-11, 08028 Barcelona, Spain

Arthur E. Martell* and Joseph Reibenspies

Department of Chemistry, Texas A&M University, College Station, Texas 77843-3255

Received July 21, 1998

The complexes $[Cu_2(dpt)_2Cl_2]X_2$ (dpt = dipropylenetriamine; X = Cl, **1**; $X_2 = (Cl)(BPh_4)$, **2**) have been prepared and their magnetic properties studied. The crystal structure of complex **1** has been solved. The compound belongs to the *C*2/*c* space group with $Z = 4$, $a = 17.201(2)$ Å, $b = 10.873(2)$ Å, $c = 11.835(2)$ Å, and $\beta = 99.720(10)°$. The geometry about each copper approximates that of a distorted square pyramid. The three N-atoms of the dpt ligand and one of the Cl bridging ligands form the base of the pyramid while the other chloro bridging ligand occupies the axial site. The two pyramids share a base-to-apex edge with the basal planes being perpendicular, an arrangement which had not been previously observed for this type of dimers. The chloro counterions are responsible for interdimer interactions through hydrogen bonding forming chains of dimers throughout the lattice. Magnetic susceptibility data show a ferromagnetic coupling between the two Cu(II) centers ($J = 42.94$ cm^{-1} for **1** and $J = 13.89$ cm^{-1} for **2**). Dimer−dimer interaction and ZFS have been considered with the J' parameter (**1**, $J' = -3.92$ cm^{-1}; **2**, $J' = -2.9$ cm^{-1}). Extended Hückel calculations on complex **1** clearly reveal that the intradimer magnetic interaction only takes place through the basal chloro bridging ligand (with a CuCl(1)Cu angle of 91.4°) which in turn is consistent with the observed ferromagnetic coupling.

Introduction

Binuclear copper(II) complexes with monatomic bridging ligands have been intensively studied over the last three decades both from a structural and a magnetic point of view.

Copper(II) complexes containing μ-OH bridging ligands with a $Cu(\mu\text{-}OH)_2Cu$ core structure are abundant and extremely similar from a structural point of view. This structural homogeneity together with the strong magnetic coupling, *J*, exhibited by this type of core has allowed the establishment of a well-behaved magneto−structural correlation.[1−5]

The replacement of the bridging hydroxy ligand by OR ligands produces structural distortions yielding complexes with different type of geometries and therefore precluding the establishment of a magneto−structural correlation based only on bond angles and distances.[3,6−8]

Binuclear copper(II) complexes containing chloro bridging ligands with a $Cu(\mu\text{-}Cl)_2Cu$ motif display a wealth of different structures with a variety of bond distances (Cu−Cl) and angles (CuClCu) depending on the coordinated ligands and also on the counterions.[9−15] As a consequence, for this type of complex the superexchange pathway depends on various orbitals, and therefore, each type of structural dimer has to be studied separately in order to draw meaningful magneto−structural correlations.

(1) Hay, P. J.; Thibeault, J. C.; Hoffmann, R. *J. Am. Chem. Soc.* **1975**, *97*, 4884.
(2) (a) Crawford, V. H.; Richardson, H. W.; Wasson, J. R.; Hodgson, D. J.; Hatfield, W. E. *Inorg. Chem.* **1976**, *15*, 2107. (b) Mitchell, T. P.; Bernard, W. H.; Wasson, J. R. *Acta Crystallogr.* **1970**, *B26*, 2096. (c) Jeter, D. Y.; Lewis, D. L.; Hempel, J. C.; Hodgson, D. J.; Hatfield, W. E. *Inorg. Chem.* **1972**, *11*, 1958. (d) Lewis, D. L.; Hatfield, W. E.; Hodgson, D. J. *Inorg. Chem.* **1972**, *11*, 2216. (e) Lewis, D. L.; McGregor, K. T.; Hatfield, W. E.; Hodgson, D. J. *Inorg. Chem.* **1974**, *13*, 1013. (f) Estes, E. D.; Hatfield, W. E.; Hodgson, D. J. *Inorg. Chem.* **1974**, *13*, 1654.
(3) Hodgson, D. J. *Prog. Inorg. Chem.* **1975**, *19*, 173.
(4) (a) McGregor, K. T.; Watkins, N. T.; Lewis, D. L.; Hodgson, D. J.; Hatfield, W. E. *Inorg. Nucl. Chem. Lett.* **1973**, *9*, 423. (b) Barnes, J. A.; Hatfield, W. E.; Hodgson, D. J. *Chem. Commun.* **1970**, 1593. (c) Casey, A. T.; Hoskins, B. F.; Whillans, F. D. *Chem. Commun.* **1970**, 904.
(5) (a) Bencini, A.; Gatteschi, D. *Inorg. Chim. Acta* **1978**, *31*, 11. (b) Countryman, R. M.; Robinson, W. T.; Sinn, E. *Inorg. Chem.* **1974**, *13*, 2013. (c) Charlot, M. F.; Kahn, O.; Jeannin, S.; Jeannin, Y. *Inorg. Chem.* **1980**, *19*, 1410.
(6) Lintvedt, R. L.; Glick, M. D.; Tomlonovic, B. K.; Gavel, D. P.; Kuszaj, J. M. *Inorg. Chem.* **1976**, *15*, 1633.
(7) (a) Bertrand, J. A.; Smith, J. H.; Eller, P. G. *Inorg. Chem.* **1974**, *13*, 1649. (b) Harris, C. M.; Sinn, E. *J. Inorg. Nucl. Chem.* **1968**, *30*, 2723. (c) Sinn, E.; Robinson, W. T. *Chem. Commun.* **1972**, 359. (d) Gluvchinsky, P.; Mockler, G. M.; Healy, P. C.; Sinn, E. *J. Chem. Soc., Dalton Trans.* **1974**, 1156. (e) Charlot, M. F.; Jeannin, S.; Jeannin, Y.; Kahn, O.; Lucrece-Abaul, J. *Inorg. Chem.* **1979**, *18*, 1675.
(8) (a) Hatfield, W. E. *Inorg. Chem.* **1972**, *11*, 216. (b) Inman, G. W.; Hatfield, W. E.; Drake, R. F. *Inorg. Chem.* **1972**, *11*, 2425. (c) Hall, D.; Sheat, S. V.; Waters, T. N. *J. Chem. Soc. A* **1968**, 460. (d) Pajunen, A.; Lehtonen, M. *Suom. Kemistil.* **1971**, *b44*, 200.
(9) (a) Hodgson, D. J.; Pedersen, E. *Acta Chem. Scand. A* **1982**, *36*, 281. (b) Rojo, T.; Arriortua, M. I.; Ruiz, J.; Darriet, J.; Villeneuve, G.; Beltran-Porter, D. *J. Chem. Soc., Dalton Trans.* **1987**, 285. (c) Blanchette, J. T.; Willett, R. D. *Inorg. Chem.* **1988**, *27*, 843. (d) Carrabine, J. A.; Sundaralingam, M. *J. Am. Chem. Soc.* **1970**, *92*, 369.

10.1021/ic9808504 CCC: $18.00
Published on Web 04/24/1999

Herein, we present the synthesis, structure and magnetic properties of a new binuclear copper(II) complex $[(dpt)Cu(\mu\text{-}Cl)_2Cu(dpt)]Cl_2$, **1**, that exhibits an unusual structure which had not been observed before for any of the $Cu(\mu\text{-}Cl)_2Cu$ complexes described to date.

Experimental Section

Materials and Reagents. Copper(II) chloride dihydrate, 99.8%, and sodium tetraphenylborate, >99.5%, were purchased from Probus. Dipropylenetriamine (dpt), 98%, was procured from Aldrich. All solvents were obtained from SDS as reagent grade and were used without further purification.

$[Cu(dpt)(Cl)]_2Cl_2$ (1). This compound was synthesized by two different routes.

Method A. A 100 mg (0.137 mmol) amount of bis(μ-chloro)-(3,7,11,19,23,27-hexaazatricyclo[27.3.1.1^{13,17}]tetratriaconta-1(32),2,11,-13(14),15,17(34),18,27,29(33),30-decaene)dicopper(II) chloride[16] was dissolved in 15 mL of methanol. Then 10 mL of water was added and the blue solution allowed to magnetically stir at room temperature for 0.5 h. The volume was then reduced to dryness and the residue dissolved in 5 mL of methanol. Addition of ether (10 mL) produced a dark blue precipitate, which was filtered off on a Büchner funnel, washed with cold methanol (5 mL) and ether (3 × 5 mL), and dried at vacuum. Yield: 42 mg (57.7%). Anal. Calcd for $C_{12}H_{34}N_6Cl_4Cu_2$: C, 27.1; H, 6.5; N, 15.8. Found: C, 27.3; H, 6.3; N, 15.7.

Method B. A solution of 500 mg (2.87 mmol) of copper chloride dihydrate in 10 mL of methanol was added to a magnetically stirred solution of 380 mg (2.87 mmols) of dpt in 10 mL of methanol. The volume of the deep blue solution formed was then reduced to about 5 mL under reduced pressure. Addition of ether (10 mL) produced a dark blue precipitate, which was filtered off on a Büchner funnel, washed with cold methanol (5 mL) and ether (3 × 5 mL), and dried at vacuum. Yield: 0.45 g (90%). Anal. Calcd for $C_{12}H_{34}N_6Cl_4Cu_2$: C, 27.1; H, 6.5; N, 15.8. Found: C, 27.1; H, 6.5; N, 15.6. IR (KBr pellet, cm^{-1}): 3241 s, 3149 s, 2931 s, 2889 s, 1595 m, 1469 w, 1434 w, 1279 m, 1152 s, 1117 s, 1082 m, 1040 s, 667 m. UV−vis (MeOH) [λ_{max}/nm (ϵ_{max}/M^{-1} cm^{-1})]: 268 (16 818), 636 (322).

$[Cu(dpt)(Cl)]_2(Cl)(BPh_4)$ (2). A solution of 130 mg (0.38 mmols) of $NaBPh_4$ in 4 mL of methanol was added to a magnetically stirred solution of 100 mg (0.19 mmol) of **1** in 6 mL of methanol. A blue precipitate appeared immediately, which was filtered off on a Büchner funnel, washed with methanol (3 × 5 mL), and dried at vacuum. Yield: 0.13 g (85%). Anal. Calcd for $C_{36}H_{54}N_6Cl_3BCu_2$: C, 53.1; H, 6.7; N, 10.3; Cl, 13.1. Found: C, 53.0; H, 6.5; N, 10.3; Cl, 13.0. IR (KBr pellet, cm^{-1}): 3304 m, 3227 s, 3051 w, 3009 w, 2924 m, 1588 s, 1462 m, 1271 m, 1152 s, 1033 s, 759 m, 709 m. UV−vis (DMF) [λ_{max}/nm (ϵ_{max}/M^{-1} cm^{-1})]: 270 (14 526), 656 (301).

Table 1. Crystal Data for the Complex $[(dpt)Cu(\mu\text{-}Cl)_2Cu(dpt)]Cl_2$ (**1**)

empirical formula	$C_{12}H_{34}N_6Cu_2Cl_4$
fw	531.3
cryst system, space group	monoclinic, *C*2/*c*
a, Å	17.201(2)
b, Å	10.873(2)
c, Å	11.835(2)
β, deg	99.720(10)
V, Å^3	2181.8(6)
formula units/cell	4
temp, K	293(2)
λ(Cu Kα), Å	1.541 78
$\rho_{calc.}$, g/cm^3	1.618
μ, mm^{-1}	7.080
R^a	0.039
$R_w{}^b$	0.045

^{a} $R = \sum|F_o - F_c|/\sum F_o$. ^{b} $R_w = \{[\sum w(F_o - F_c)^2]/[\sum w(F_o)^2]\}^{1/2}$.

Measurements and Calculations. C, H, and N elemental analyses were performed by SIR-UdG (Integrated Research Services from the University of Girona) with a Fissons instrument whereas Cl analyses were done by following Volhard's method.[17] Infrared spectra were obtained on a Nicolet 205 FT-IR spectrophotometer using KBr pellets. Absorption spectra were recorded on a diode-array Hewlett-Packard HP-89532A UV−vis spectrophotometer. EPR spectra were monitored with a Bruker ESP 300E. Samples were run at 9.4 GHz (X-band) in the temperature range 4−298 K. EPR simulations were performed using the WIN-EPR Simfonia program from Bruker. For complex **1**, variable-temperature magnetic susceptibility measurements in the polycrystalline state were carried out on a Quantum Design MPMS SQUID equipped with a 55 kG magnet in the temperature range 1.8−300 K with an applied magnetic field of 15 000 G. For complex **2**, variable-temperature magnetic susceptibility measurements in the polycrystalline state were carried out on a MANIC DSM8 equipped with a Bruker BE15 electromagnet and an Oxford CF 1200S cryogenic apparatus. Data were taken in the temperature range 4−300 K with an applied magnetic field of 15 000 G. Diamagnetic corrections were estimated from Pascal tables. Powder X-ray diffraction analysis were carried out in an Siemens D500 automatic diffratometer. Molecular orbital calculations were carried out using CACAO 4.0 (computer-aided composition of atomic orbitals),[18] a program based on the extended Hückel type of analysis.

Crystallographic Measurements. A blue needle was mounted on a glass fiber with epoxy cement, at room temperature. Preliminary examination and data collection was performed on a Rigaku AFC5R X-ray diffractometer (oriented graphite monochromator; λ(Cu Kα) = 1.541 78 Å radiation). Data were collected using the $\theta-2\theta$ scan mode for $4.0° \le 2\theta \le 120.0°$ at 293 K. The structure was solved by direct methods, and full-matrix least-squares anisotropic refinement was used for all non-hydrogen atoms (SHELXS, SHELXTL-PLUS program package[19]). Hydrogen atoms were placed in idealized positions with isotropic thermal parameters fixed at 0.08 Å^2. Neutral atom scattering factors and anomalous scattering correction terms were taken from ref 20. A summary of the data collection and structure solution is given in Table 1.

Results and Discussion

Synthesis and Structure. The binuclear copper complex $[(dpt)Cu^{II}(\mu\text{-}Cl)_2Cu^{II}(dpt)]Cl_2$, **1**, was originally obtained from hydrolysis of a hexaaza Schiff base macrocyclic binuclear complex as shown in eq 1,

(10) (a) Hodgson, D. J.; Hale, P. K.; Hatfield, W. E. *Inorg. Chem.* **1971**, *10*, 1061. (b) Søtofte, I.; Nielsen, K. *Acta Chem. Scand. A* **1981**, *35*, 733.(c) Tosik, A.; Maniukievicz, W.; Bukowska-Strzyzewska, M.; Mrozinski, J.; Sigalas, M. P.; Tsipis, C. A. *Inorg. Chim. Acta* **1991**, *190*, 193. (d) Hoffmann, S. K.; Hodgson, D. J.; Hatfield, W. E. *Inorg. Chem.* **1985**, *24*, 1194. (e) Swank, D. D.; Needham, G. F.; Willett, R. D. *Inorg. Chem.* **1979**, *18*, 761.

(11) Brown, S. J.; Tao, X.; Wark, T. A.; Stephan, D. W.; Mascharak, P. K. *Inorg. Chem.* **1988**, *27*, 1581.

(12) (a) Sheldrick, W. S. *Acta Crystallogr., Sect. B: Struct. Crystallogr. Cryst. Chem.* **1981**, *B37*, 945. (b) Brown, D. B.; Hall, J. W.; Helis, J. M.; Walton, E. G.; Hodgson, D. J.; Hatfield, W. E. *Inorg. Chem.* **1977**, *16*, 2675. (c) Graf, M.; Greaves, B.; Stoeckli-Evans, H. *Inorg. Chim. Acta* **1993**, *204*, 239. (d) Honda, M.; Katayama, C.; Tanaka, J.; Tanaka, M. *Acta Crystallogr.* **1985**, *C41*, 688. (e) *Acta Crystallogr.* **1985**, *C41*, 197. (f) Willett, R. D.; Dwiggins, C.; Kruh, R. F.; Rundle, R. E. *J. Chem. Phys.* **1963**, *38*, 2429.

(13) (a) Colombo, A.; Menabue, L.; Motori, A.; Pellacani, G. C.; Porzio, W.; Sandrolini, F.; Willett, R. D. *Inorg. Chem.* **1985**, *24*, 2900. (b) Scott, B.; Geiser, U.; Willett, R. D.; Patyal, B.; Landee, C. P.; Greeney, R. E.; Manfredini, T.; Pellacani, G. C.; Corradi, A. B.; Battaglia, L. P. *Inorg. Chem.* **1988**, *27*, 2454. (c) Willett R. D. In *Magneto-structural correlations in exchange coupled systems*: Gatteschi, D., Kahn, O., Willett, R. D., Eds.; NATO Advanced Study Institute Series Vol. C140; D. Reidel: Dordrecht, Holland, 1984.

(14) (a) Marsh, W. E.; Patel, K. C.; Hatfield, W. E.; Hodgson, D. J. *Inorg. Chem.* **1983**, *22*, 511. (b) Marsh, W. E.; Eggleston, D. S.; Hatfield, W. E.; Hodgson, D. J. *Inorg. Chim. Acta* **1983**, *70*, 137.

(15) Roundhill, S. G. N.; Roundhill, D. M.; Bloomquist, D. R.; Landee, C.; Willett, R. D.; Dooley, D. M.; Gray, H. B. *Inorg. Chem.* **1979**, *18*, 831.

(16) Llobet, A.; Martell, A. E.; Martínez, M. A. *J. Mol. Catal.* **1998**, *129*, 19−26.

(17) Volhard, J. *J. Prakt. Chem.* **1874**, *117*, 217.

(18) Mealli, C.; Proserpio, D. M. *J. Chem. Educ.* **1990**, *67*, 399.

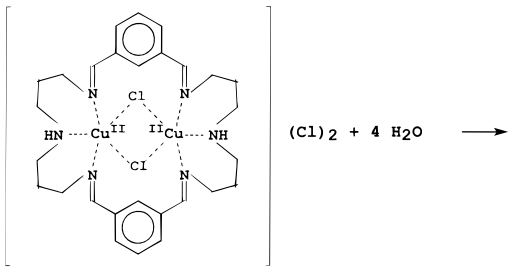

$$[(dpt)Cu^{II}(\mu\text{-}Cl)_2Cu^{II}(dpt)]Cl_2 \quad + \quad 2\ m\text{-}Ph(CHO)_2 \quad (1)$$
1

However, **1** can also be easily obtained by mixing equimolecular amounts of $CuCl_2$ and dpt in methanol,

$$2Cu^{II}Cl_2 + 2dpt \xrightarrow{MeOH} \underset{\mathbf{1}}{[(dpt)Cu^{II}(\mu\text{-}Cl)_2Cu^{II}(dpt)]Cl_2} \quad (2)$$

Complex **1** has the same crystallographic structure irrespectively of the synthetic method used to prepare it as has been proved by powder X-ray diffraction analysis.

Addition of excess $NaBPh_4$ to a methanolic solution of **1** produces $[(dpt)Cu^{II}(\mu\text{-}Cl)_2Cu^{II}(dpt)](Cl)(BPh_4)$, **2**, with the substitution of only one Cl^- counterion. Table 1 contains crystallographic data for complex **1** whereas Table 2 contains selected bond distances and angles. Figure 1 displays the ORTEP diagram obtained for the molecular structure of complex **1** that crystallizes in the monoclinic space group *C*2/*c* with four molecules per unit cell. The complex ion possesses 2-fold symmetry, with the bridging chlorides lying on the C_2 axis. Complex **1** contains two pentacoordinate copper metal ions which are bridged by the two chloro ligands while the other three positions are filled by the amino nitrogens of a dpt ligand. For this complex, bond distances and angles are relatively similar to those reported for related complexes.[9b,11,15,21]

Each Cu has a distorted square pyramidal type of geometry as ascertained by Reedijk's[22] τ factor of 0.355 ($\tau = 0$ for a square pyramid, and $\tau = 1$ for a trigonal bipyramid)

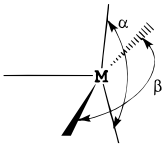

$$\tau = \frac{\alpha - \beta}{60}$$

and are related to one another by a C_2 axis which crosses through the Cl bridging ligands. The nitrogen atoms of a dpt ligand N(1a), N(2a), and N(3a) and the chloro bridging ligand Cl(1) are nearly coplanar constituting the base of the pyramid whereas the other chloro bridging ligand Cl(2) occupies the apical position. The Cu(1a) metal atom lies roughly 0.27 Å above the basal plane. The other copper metal atom Cu(1) shares Cl(1) for the base and Cl(2) for the apical position. As a result, the geometry of the complex consists of two square pyramids sharing one base-to-apex edge with the two bases nearly perpendicular to one another (type I structure shown) with a CuCl(1)Cu angle of 91.4°.

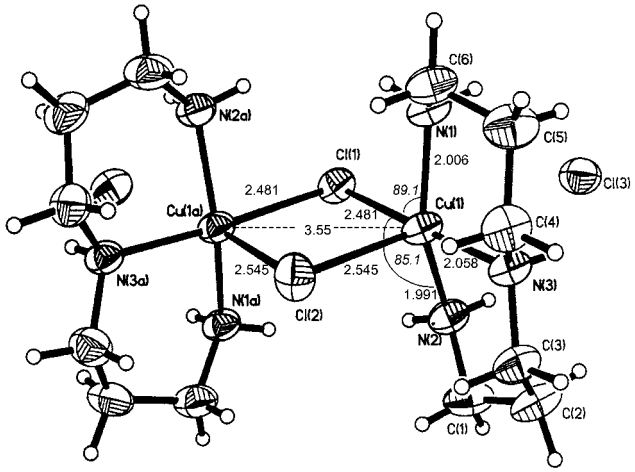

Figure 1. ORTEP view of the molecular structure of $[(dpt)Cu(\mu\text{-}Cl)_2Cu(dpt)](Cl)_2$ (**1**) (50% probability).

Table 2. Selected Bond Lengths (Å) and Bond Angles (deg) for the Complex $[(dpt)Cu(\mu\text{-}Cl)_2Cu(dpt)]Cl_2$ (**1**)

Cu(1)−Cl(1)	2.481(1)	Cu(1a)−Cl(1)	2.481(1)
Cu(1)−Cl(2)	2.545(2)	Cu(1a)−Cl(2)	2.545(2)
Cu(1)−N(1)	2.006(4)	Cu(1)−N(2)	1.991(4)
Cu(1)−N(3)	2.058(4)	Cu(1)−Cu(1a)	3.551
Cu(1)−Cl(3)	3.128	N(1)−C(6)	1.476(7)
N(2)−C(1)	1.476(7)	N(3)−C(3)	1.488(6)
N(3)−C(4)	1.484(6)	C(1)−C(2)	1.486(9)
C(2)−C(3)	1.503(7)	C(4)−C(5)	1.498(7)
C(5)−C(6)	1.508(8)		

Cl(1)−Cu(1)−Cl(2)	90.1(1)	Cl(1)−Cu(1)−N(1)	89.1(1)
Cl(2)−Cu(1)−N(1)	98.9(1)	Cl(1)−Cu(1)−N(2)	85.1(1)
Cl(2)−Cu(1)−N(2)	106.6(1)	N(1)−Cu(1)−N(2)	153.8(2)
Cl(1)−Cu(1)−N(3)	175.1(1)	Cl(2)−Cu(1)−N(3)	94.5(1)
N(1)−Cu(1)−N(3)	91.9(2)	N(2)−Cu(1)−N(3)	91.9(2)
Cu(1)−Cl(1)−Cu(1a)	91.4(1)	Cu(1)−Cl(2)−Cu(1a)	88.5(1)
Cu(1)−N(1)−C(6)	119.3(3)	Cu(1)−N(2)−C(1)	122.3(3)
Cu(1)−N(3)−C(3)	115.0(3)	Cu(1)−N(3)−C(4)	115.7(3)
C(3)−N(3)−C(4)	108.4(4)	N(2)−C(1)−C(2)	111.3(4)
C(1)−C(2)−C(3)	114.2(5)	N(3)−C(3)−C(2)	112.9(4)
N(3)−C(4)−C(5)	114.4(4)	C(4)−C(5)−C(6)	114.4(5)
N(1)−C(6)−C(5)	111.0(4)		

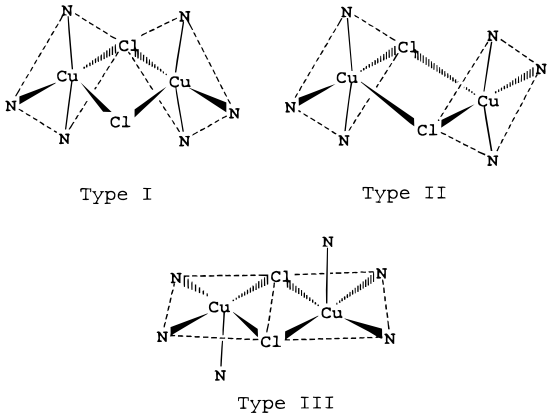

The present case constitutes the first example of a binuclear copper complex with two chloro bridges and a tridentate N-donor ligand where the two square pyramids have this type of arrangement.

Two main other types of pyramidal arrangements are found in the literature: (a) square pyramids sharing one base-to-apex

(19) Sheldrick, G. M. *SHELXTL-PLUS (4.11), an integrated system for solving, refining and displaying crystal structures from diffraction data*; Institüt für Anorganishe Chemie der Universität: Tammannstrasse 4, D-3400 Gottingen, Germany, 1990.
(20) International Tables for X-ray Crystallography; Ibers, J. A., Hamilton, W. C., Eds.; Kynoch Press: Birmingham, England, 1974; Vol IV, pp 99, 149.
(21) Hoffmann, S. K.; Towle, D. K.; Hatfield, W. E.; Wieghardt, K.; Chaudhuri, P.; Weiss, J. *Mol. Cryst. Liq. Cryst.* **1984**, *107*, 161.
(22) Addison, A. W.; Rao, T. N.; Reedijk, J.; Rijn, J. V.; Verschoor, G. C. *J. Chem. Soc., Dalton Trans.* **1984**, 1349.

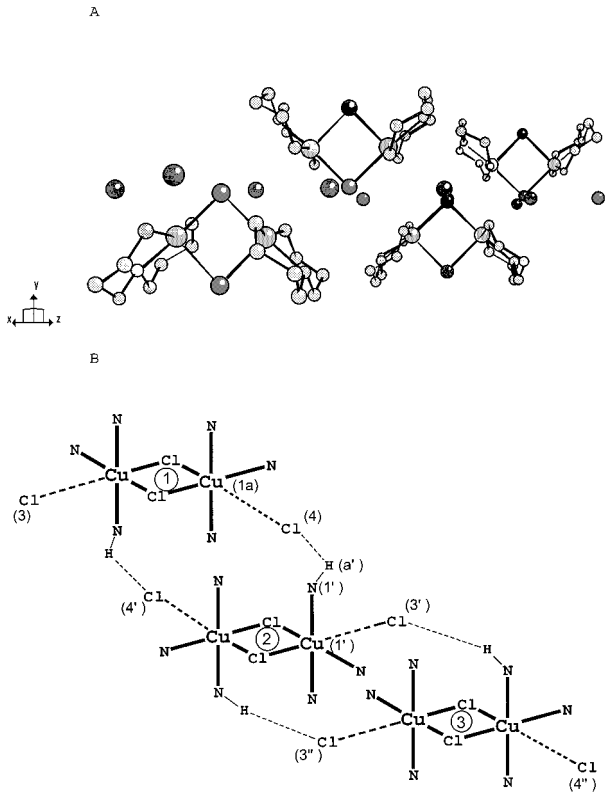

Figure 2. (A) View of the chain structure in the crystal lattice of complex **1**. Cl counterions are responsible linking each dimer to one another through hydrogen bonding. (B) Schematic representation where dotted lines represent hydrogen bonding and anionic chloride−copper interactions.

edge but with parallel basal planes (type II);[10c,14a,21,23] (b) square pyramids sharing a basal edge with coplanar basal planes (type III).[24−27,28a] The distances Cu(1)−N(1) (2.006(4) Å) and Cu(1)−N(2) (1.991(4) Å) are relatively similar and slightly shorter than that of the Cu1−N(3) (2.058(4) Å) which is the nitrogen atom trans to the basal chloro ligand.

With regard to the Cu(μ-Cl_2)Cu core, the distance between the copper metal center and the apical chloro ligands (Cu(1)−Cl(2), 2.545(2) Å) is slightly larger than that of the copper and the basal chloro ligands (Cu(1)−Cl(1), 2.481(1) Å) with the ClCuCl bond angles being 90.1(1)°. As a consequence the other two cores angles are significantly different: the "basal" core angle CuCl(1)Cu is 91.4(1)°, and the "apical" core angle CuCl-(2)Cu is 88.5(1)°. Therefore the Cu(μ-Cl_2)Cu core has an asymmetric rhomboidal geometry with a Cu−Cu distance of 3.550 Å.

Finally, chloride counterions are situated trans with respect to the apical chloro ligands at a distance of 3.129 Å from the metal center (more than 0.58 Å higher than the covalent Cl bridging ligands).

In the crystal structure, the dimers interact with one another through anionic Cl interactions and hydrogen bonding forming chains as depicted in Figure 2. Each dimer is linked to two other dimers through four symmetrical Cu−Cl−H−N−Cu interactions (a distance of 2.510 Å is observed for the Cl−H bond). Those interactions implicate all the ionic Cl atoms through the whole structure, while the Cl ligands that bridge

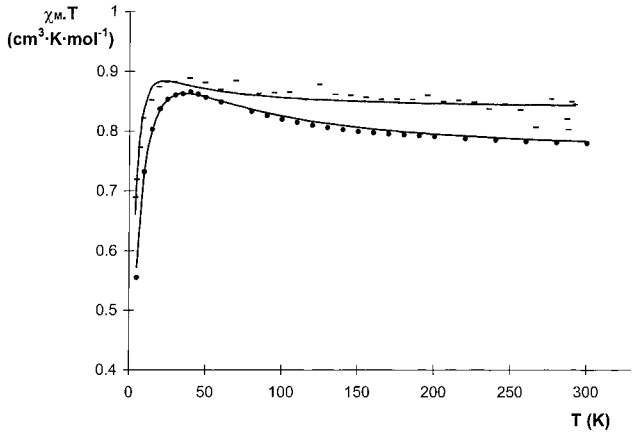

Figure 3. $\chi_M T$ vs T experimental data for **1** (●) and **2** (—) (cm^3·K·mol^{-1}). Solid lines show the best fit obtained (see text).

the Cu metal atoms are not involved in the interdimer interactions. Each dpt ligand has one N atom involved in the hydrogen bonding which is perpendicular to the Cu_2Cl_2 core and is symmetrically related to its counterpart on the other dpt ligand.

Magnetic Properties. Figure 3 presents a graph of the molar $\chi_M T$ product vs T for compounds **1** and **2**. For **1**, at 298 K the value of $\chi_M T$ is 0.779 cm^3·K·mol^{-1} and increases continuously as the temperature decreases giving a maximum value of 0.865 cm^3·K·mol^{-1} at 40 K manifesting a ferromagnetic coupling between the two Cu(II) metal centers. A similar trend is observed for **2** with a value of $\chi_M T$ of 0.843 cm^3·K·mol^{-1} at 292 K and a maximum of 0.889 cm^3·K·mol^{-1} at 39.5 K. Below the maximum, $\chi_M T$ decreases as the temperature decreases in both cases which is indicative of an interdimer antiferromagnetic coupling, zero-field splitting (ZFS), or a mixture of both. To fit also the decrease of $\chi_M T$ at low temperature, the new parameter J' had to be introduced. Thus, the experimental data were fitted using the following Bleany−Bowers equation for a binuclear compound with a total spin $S = 1$ containing the J' term,

$$\chi_M = \frac{2N\beta^2 g^2}{kT - (2J'\ 3 + \exp(-J/kT))}[3 + \exp(-J/kT)]^{-1}$$

The fit was performed by minimizing the function $R = \Sigma-(\chi_M T_{calc} - \chi_M T_{obs})^2/\Sigma(\chi_M T_{obs})^2$, the best fit parameters being $J = 42.94$ cm^{-1}, $J' = -3.92$ cm^{-1}, and $g = 2.04$ with $R = 4.45 \times 10^{-5}$ for **1** and $J = 13.89$ cm^{-1}, $J' = -2.9$ cm^{-1}, and $g = 2.11$ with $R = 2.83 \times 10^{-4}$ for **2**.

Magnetization experiments (Figure S1) carried out for complex **1** at 2 K up to a field of 50 000 G show a progressive magnetization increase as the applied magnetic field increases which is consistent with a $S = 1$ ground state. As the applied field decreases to −1000 G the magnetization also decreases without inducing any permanent magnetization. Magnetization experiments at 300 K from 5000 to −5000 G also reveal the absence of a hysteresis cycle for complex **1**.

Figures 4 and 5 display the powder electron paramagnetic resonance (EPR) spectra obtained at 289 and 4 K and their mathematical simulation for compounds **1** and **2**, respectively.

For **1**, the EPR spectrum at 298 K consists of a single asymmetric band centered at $g = 2.1$ with a 200 G line width. At 4 K the EPR shows two signals: one at $g_1 = 2.17$ and a second one less intense at $g_2 = 2.07$ with line widths of 40 and 90 G, respectively. At higher temperatures ($T = 298$ K) the spectrum is less intense than at lower temperatures which is again consistent with a triplet ground state for the dimer. No

(23) (a) Megnamisi-Bélombé, M.; Novotny, M. A. *Inorg. Chem.* **1980**, *19*, 2470. (b) Phelps, D. W.; Goodman, W. H.; Hodgson, D. J. *Inorg. Chem.* **1976**, *15*, 2266. (c) Estes, E. D.; Estes, W. E.; Hatfield, W. E.; Hodgson, D. J. *Inorg. Chem.* **1975**, *14*, 106. (d) O′Connor, C. J. *Inorg. Chim. Acta* **1987**, *127*, L29.

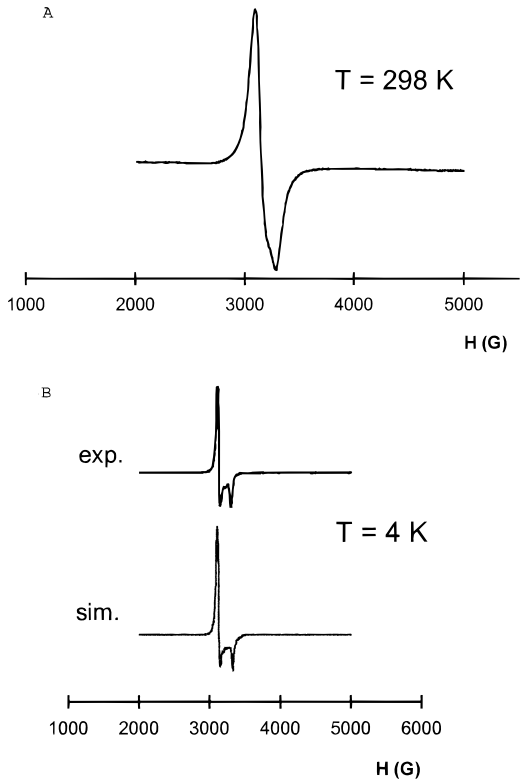

Figure 4. (A) EPR spectrum at 298 K for complex **1**. (B) EPR spectrum at 4 K for complex **1** and its mathematical simulation.

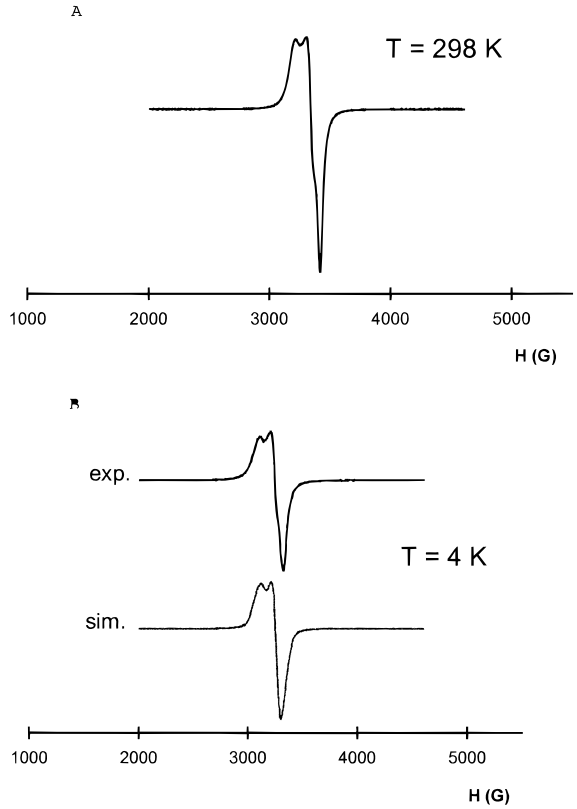

Figure 5. (A) EPR spectrum at 298 K for complex **2**. (B) EPR spectrum at 4 K for complex **2** and its mathematical simulation.

absorption is observed at half-field ($\Delta m_s = 2$; $g = 4$) indicating a small ZFS effect.[29]

Figure 4B displays the simulated EPR spectrum of **1** at 4 K using $g_x = 2.17$, $g_y = 2.10$, and $g_z = 2.07$, $D = 106$ G (9.91 10^{-3} cm^{-1}), $E = 32$ G (2.99 10^{-3} cm^{-1}), and a hyperfine coupling constant for the two Cu, $A_{zz} = 25$ G. With these parameters Wasserman's et al. equation for a triplet ground state[30] yields the following six $\Delta M_s = 1$ transitions: $H_{x1} = 3103.41$ G, $H_{y1} = 3115.80$ G, $H_{z1} = 3156.17$ G, $H_{x2} = 3112.64$ G, $H_{y2} = 3308.41$ G, and $H_{z2} = 3361.24$ G.

For **2**, the EPR spectrum at 298 K consists of one asymmetric band centered at $g_1 = 2.08$ with a bandwidth of 125 G and a second band with less resolution at $g_2 = 2.18$. Lowering the temperature to 4 K produces an increase of band intensity, but the shape of the spectrum remains practically constant.

Figure 5B displays the simulated EPR spectrum of **2** at 4 K using $g_x = 2.07$, $g_y = 2.09$, and $g_z = 2.13$, $D = 112$ G (1.05 10^{-2} cm^{-1}), $E = 35$ G (3.27 10^{-3} cm^{-1}), and $A_{zz} = 16$ G. With these parameters the six transitions are found at $H_{x1} = 3258.14$ G, $H_{y1} = 3126.92$ G, $H_{z1} = 3064.95$ G, $H_{x2} = 3262.92$ G, $H_{y2} = 3334.83$ G, and $H_{z2} = 3275.53$ G.

For ferromagnetic systems with $S = 1$ at room temperature the EPR spectrum is the sum of 4 transitions ($S = 0$, 1 populated) with the three x, y, and z components for each one. At 4 K, for systems with $J > 3$ cm^{-1}, only the $S = 1$ state is significantly populated and thus only two transitions are expected. In our case at 4 K (see Figures 4B and 5B) complex **1** displays a higher spectrum resolution than complex **2**. This is due to the fact that small differences in the g_i, D, E, and A_{zz} parameters can substantially modify the shape of the spectrum.

For both complexes, the simulated ZFS parameters D and E are relatively similar. The bigger one, D (approximately 0.01 cm^{-1}), is more than 2 orders of magnitude smaller than J' (approximately 3−4 cm^{-1}) in either case which agrees with the hypothesis that ZFS is practically negligible.

From the magnetic results, EPR experiments, and the crystal structure one can infer that, in complex **1**, there is an intradimer ferromagnetic coupling between the Cu(II) metal centers through the chloro bridging ligands ($J = 42.94$ cm^{-1}) and an weaker interdimer antiferromagnetic coupling ($J' = -3.92$ cm^{-1}) which presumably takes place through the hydrogen bonding network established by the anionic chloro counterions.

The lack of a crystal structure for complex **2** prevents an incontestable interpretation of its magnetic properties. However, complex **2** is also ferromagnetic but with a smaller J value ($J = 13.89$ cm^{-1}) than for complex **1**. Its EPR spectrum at 4 K is relatively similar to what is found for complex **1** with very close g values but with reversed intensities. Thus, one can speculate that these differences in magnetic behavior might be due to small changes into the core structural parameters.

Molecular Orbital Calculations and Magneto−Structural Correlations. Extended Hückel calculations[18] for **1** have been performed in order to gain insight into the molecular orbitals that participate in the superexchange pathway.

Using the crystallographic coordinates for the cationic dimer $[(dpt)Cu^{II}(\mu\text{-}Cl)_2Cu^{II}(dpt)]^{2+}$ a small energy difference of 0.47 eV is obtained between the HOMO and LUMO which in turn are about 1.5 eV above occupied orbitals. The calculations

(24) Textor, M.; Dubler, E.; Oswald, R. *Inorg. Chem.* **1974**, *13*, 1361.
(25) Willett, R. D.; Chow, C. *Acta Crystallogr., Sect. B* **1974**, *30*, 207.
(26) O'Brien, S.; Gaura, R. M.; Landee, C. P.; Ramakhrishna, B. L.; Willett, R. D. *Inorg. Chim. Acta* **1988**, *141*, 83.
(27) Chow, C.; Willett, R. D.; Gerstein, B. C. *Inorg. Chem.* **1975**, *14*, 205.
(28) (a) Roberts, S. A.; Bloomquist, D. R.; Willett, R. D.; Dodgen, H. W. *J. Am. Chem. Soc.* **1981**, *103*, 2103. (b) Inoue, M.; Kishita, M.; Kubo, M. *Inorg. Chem.* **1967**, *6*, 900.
(29) Lucas, R.; Liu, S.; Thompson, L. K. *Inorg. Chem.* **1990**, *29*, 85.
(30) Wasserman, E.; Snyder, L. C.; Yager, W. A. *J. Chem. Phys.* **1964**, *41*, 1763.

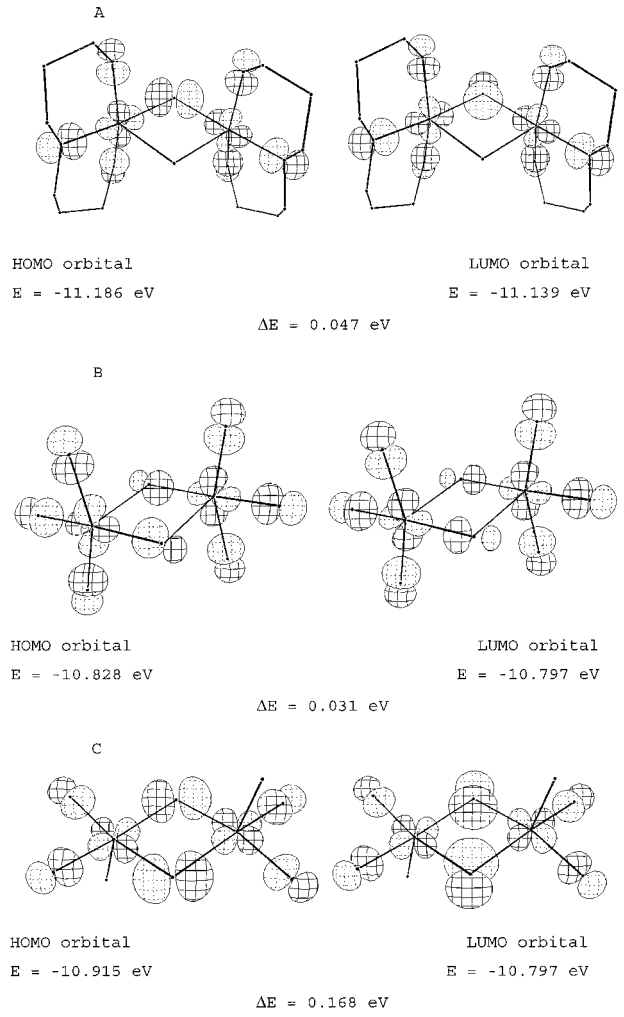

Figure 6. Drawings of the HOMO and LUMO frontier orbitals (for orbitals contributing more than 1%) obtained for (A) the cation of complex **1**, $[(dpt)Cu(\mu\text{-}Cl)_2Cu(dpt)]^{2+}$, belonging to type I symmetry, (B) an example of type II symmetry, and (C) an example of type III symmetry (see text for details in this and the previous case).

indicate the following orbital participation: Cu d orbitals, 40%; N p orbitals, 5%; Cl p orbitals from Cl(1), 12−14%. It is interesting to note that the contribution to frontier orbitals of Cl(2), the apical chloro ligand, is less than 1%.

A graph of the HOMO and LUMO orbitals for complex **1** is depicted in Figure 6A. As it can be observed, the Cu metal centers use $d_{x^2-y^2}$ type orbitals for a σ^* interaction with p_N and p_{Cl} orbitals. The LUMO orbital is a symmetric $d_{Cu}-d_{Cu}$ orbital combination whereas the HOMO orbital is a $d_{Cu}-d_{Cu}$ antisymmetric combination. The CuCl(1)Cu angle is very close to 90° ($\alpha = 91.4°$); as a result, the overlap between $d_{Cu}-p_{Cl(1)}-d_{Cu}$ is very similar for both frontier orbitals thus yielding relatively close energies. This similarity of energies for the HOMO and LUMO orbitals is in turn consistent with the ferromagnetic behavior[1] displayed by the complex.

The results of EH calculations described above clearly show that Cl(2) does not participate in the superexchange pathway and therefore the ferromagnetic coupling takes place through the CuCl(1)Cu path. This result is a direct consequence of the special geometry presented by complex **1**. For complexes with other geometries (types II and III) the superexchange pathway takes place through both Cl bridging ligands (Figure 6B and 6C). For type II complexes (parallel square bases) EH calculations were performed using the structural parameters from the

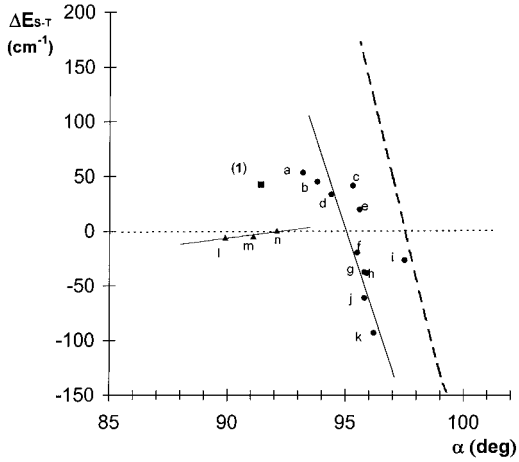

Figure 7. Magneto−structural correlation diagram for some binuclear Cu(II) complexes bridged by two chloro ligands (see Table 3 for data).

Table 3. Magneto−Structural Correlation Parameters for Selected Binuclear Copper Complexes Containing the $Cu(\mu\text{-}Cl)_2Cu$ Core

	compd[a]	geometry type	α	ΔE_{S-T}, cm^{-1}	ref
a	$(Ph_4P)_2[Cu_2Cl_6]$	III	93.2	53.4	19
b	$(Ph_4As)_2[Cu_2Cl_6]$	III	93.8	45.1	20
c	$(4\text{-}BzpipdH)_2[Cu_2Cl_6]$	III	95.3	41.7	21
d	$[Cu_2Cl_2(HB(1\text{-}pz)_3)_2]$	III	94.4	33.7	15
e	$(Me_2NH_2)_2[Cu_2Cl_6]$	III	95.6	≈20	22
f	$(i\text{-}PrNH_3)_2[Cu_2Cl_6]$	III	95.5	−19.46	23a
g	$(melH_2)[Cu_2Cl_6]$	III	95.8	−37.53	13a
h	$K_2[Cu_2Cl_6]$	III	95.9	−38.23	23b
i	$(paraquat)[Cu_2Cl_6]$	III	97.5	−26.41	21
j	$(morphH)_2[Cu_2Cl_6]$	III	95.8	−61.16	13b
k	$(DBTTF)[Cu_2Cl_6]$	III	96.2	−93.12	12d
l	$[Cu_2(terpy)_2Cl_2][PF_6]_2$	II	89.9	−5.9	9b
m	$[Cu_2(Pypep)_2Cl_2]\cdot 2H_2O$	II	91.1	−4.6	11
n	$[Cu_2(dien)_2Cl_2](ClO_4)_2$	II	92.1	0.4	16
1	$[Cu_2(dpt)_2Cl_2]Cl_2$	I	91.4	42.94	this work

[a] Ligand abbreviations: 4-BzpipdH, 4-benzilpiperidinic cation; HB(1-pz)$_3$, hydrotris(1-pyrazolyl)borate; i-Pr, isopropyl; $melH_2$, melaminic cation, $C_3H_2N_3(NH_2)_3^{2+}$; paraquat, 1,1′-dimethyl-4,4′-bipyridinic cation; morphH, mopholinic cation (tetrahydro-1,4-oxazinic); DBTTF, dibenzotetrathiafulvalenic cation; trpy, 2,2′:6′,2″-terpyridine; Pypep, piperidinic cation, *N*-(2-(4-imidazolyl)ethyl)-2-pyridine-2-carboxamidic; dien, diethylenetriamine.

X-ray crystal structure of the binuclear complex $[Cu_2(trpy)_2Cl_2](PF_6)_2$[9b] (trpy is 2,2′:6′,2″-terpyridine) but substituting the trpy ligands by amino ligands. The pattern for the orbitals energy obtained using EH calculations is similar to the previous case in the sense that there is a small energy gap between frontier orbitals (0.031 eV) and those are well above (1.793 eV) fully occupied orbitals. A graph of the HOMO and LUMO orbitals for this case is depicted in Figure 6B. As can be observed the Cu metal centers use $d_{x^2-y^2}$ orbitals for a σ^* interaction with the p_N and p_{Cl} orbitals of the base. As in the previous case, the HOMO is an antisymmetric combination of $d_{Cu}-d_{Cu}$ orbitals whereas the LUMO is the symmetric one. The superexchange pathway with the metal centers will take place mainly through a π^* type of interaction between the Cu $d_{x^2-y^2}$ and the apical p_{Cl} orbitals. For an ideal geometry with a square core the former overlap integral would be zero, and therefore, there would be no magnetic coupling between the Cu metals. As a consequence of the above, these type II complexes present very small *J* values (see Figure 7) which are due to small structural deviations from the ideal squared Cu_2Cl_2 core.

For type III complexes (coplanar square bases) EH calculations were performed using the structural parameters from the

X-ray crystal structure of the binuclear complex $[Cu_2(tpb)_2Cl_2]$[15] (tpb is tris(1-pyrazolyl)borate) but substituting the tpb ligands by amino ligands. The pattern for the orbitals energy obtained using EH calculations is again similar to the previous cases; there is a small energy gap between frontier orbitals (0.148 eV), and those are well above (1.577 eV) fully occupied orbitals. A graph of the HOMO and LUMO orbitals for this case is depicted in Figure 6C. As it can be observed the Cu metal centers use $d_{x^2-y^2}$ orbitals for a σ^* interaction with the p_N and p_{Cl} orbitals of the base. In this case both Cl bridging ligands are situated in the base of the pyramid, and therefore, both of them contribute significantly to the superexchange pathway between the copper metal centers. Within this geometry, an ideally squared Cu_2Cl_2 core would provoke a frontier orbitals degeneracy.

Structure and magnetic data are presented in Figure 7 for all dimers containing N-based ligands, $N_3Cu(\mu\text{-}Cl)_2CuN_3$, and for $[Cu_2Cl_6]^{2+}$ complexes.

The plot of $2J$ vs α (shortest CuClCu angle) shows that dimers with the same type of structure correlate relatively well. Complexes having type III structure (square planar pyramids sharing a basal edge) are gathered close to a straight line with a slope of -48.65 cm^{-1}/deg that passes through $2J = 0$ at 95.1° (the analogous curve for hydroxide-bridge square planar dimers has a slope of about -79.93 cm^{-1}/deg and passes through $2J = 0$ at 97.6°).[3] $[Cu_2Cl_6]^{2+}$ complexes with slightly distorted type III structures display a small deviation from the magneto−structural correlation as can be observed in Figure 7. These distortions arise since the plane formed by the coppers and the nonbridging chlorines are tilted with respect to the plane of the copper and the bridging chlorines. Broad deviations from the magneto−structural correlation are due to either because of uncertainties in the exchange constant or because of changes in the coordination geometry.[15]

Type II complexes (two square pyramids sharing a base-to-apex edge with parallel basal planes) also correlate relatively well with a line of 2.82 cm^{-1}/deg that passes $2J = 0$ at 92.2°. Given the relatively small span of α angles and small magnetic coupling constants, more complexes possessing this symmetry are needed in order to report a more accurate and reliable slope and intercept values.

Complex **1**, which has a type I structure (two square pyramids sharing a base-to-apex edge with perpendicular basal planes), is clearly out of any of the correlation lines drawn in Figure 7, as expected, since its structure is different from any of the complexes known to date. From a magnetic point of view, the behavior of complex **1** would be equivalent to a binuclear copper complex bridged by only one Cl ligand. In that case, steric effects would lead to a significant opening of the CuClCu angle that would bring about an important energy difference between the HOMO and LUMO orbitals described above. Significant bending of the CuCl(1)Cu angle will provoke a strong destabilization of the HOMO orbital whereas the opposite will happen to the LUMO orbital. As a consequence this hypothetical complex would have a strong intradimer antiferromagnetic coupling.

In conclusion, new binuclear complexes with chloro bridging ligands have been prepared and structurally and magnetically characterized. Chloro atoms in complex **1** play a key role both from a structural and a magnetic viewpoint. The basal chloro bridging ligand Cl(1) atom is responsible for the superexchange pathway between the Cu(II) metal centers that produces the ferromagnetic behavior. The apical chloro bridging ligand Cl(2), although not participating in the superexchange pathway, is responsible for overcoming the steric hindrance that would otherwise exist in the case of a monobridged dimer and therefore is indirectly responsible for the type of magnetic behavior observed. Finally the Cl counterions are responsible for the formation of a hydrogen bonding network which builds a dimer chain through the crystal lattice. This hydrogen bonding interaction accounts for the interdimer antiferromagnetic coupling which is predominant at lower temperatures.

Future Prospects. Complex **1** constitutes an example of the so-called "spin-ladder",[31] that is dimers which are stacked above one another with each metal ion having one interaction to the partner on the same level ($J_1 = 43$ cm^{-1}, ferromagnetic in this complex) and then a separate antiferromagnetic interaction, $J_2 = -3.2$ cm^{-1}, with the ions above and below the ladder. The antiferromagnetic interaction between dimers will generate a spin singlet for the ground state. Theoretical studies for spin ladders[31b] predict an energy gap for the ground state ($S' = 0$) and the other states with S' different from zero. This energy gap is proportional to J_2, so it will only be about 1 or 2 cm^{-1} for this compound. However, at the lowest temperatures, the susceptibility should go to zero and the magnetization curve should start up at a very low value and then suddenly jump as the gap is closed. With our present low-temperature data it is not possible to tell if there is evidence or not for such behavior. We are at present performing further magnetization experiments at low temperatures in order to get reliable data to confirm or not the above-mentioned behavior. This is particularly interesting since complex **1** is the first example of a ferromagnetic dinuclear copper complex with a "spin-ladder" disposition and moderate interactions.

Acknowledgment. This research has been supported by the DGICYT of Spain through grants PB96-0467 and PB96-0163 and by the Robert A. Welch Foundation under Grant No. A259. The CIRIT of Catalunya is also gratefully acknowledged for an aid SGR-3102-UG-01 and for the allocation of an FI doctoral grant to M.R.

Supporting Information Available: Figure S1, containing magnetization experiment data at 2, 20, and 300 K for complex **1**, and an X-ray crystallographic file, in CIF format, for **1**. This material is available free of charge via the Internet at http://pubs.acs.org.

IC9808504

(31) (a) Chiari, B.; Helms, J.; Piovesana, O.; Tarantelli, T.; Zanazzi, P. F. *Inorg. Chem*. **1986**, *25*, 870−874. (b) Dagotto, B.; Rice, T. M. *Science* **1996**, *271*, 618−623.